IC/94/353

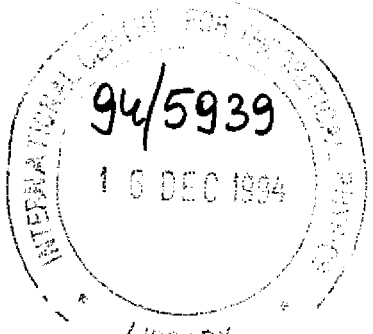

INTERNATIONAL CENTRE FOR THEORETICAL PHYSICS

CRITICAL TEMPERATURES T_c ESTIMATED BY JOSEPHSON-JUNCTION ARRAY MODEL OF LAYERED HIGH T_c SUPERCONDUCTORS

C. Kawabata

S.R. Shenoy

and

A.R. Bishop

INTERNATIONAL ATOMIC ENERGY AGENCY

UNITED NATIONS EDUCATIONAL, SCIENTIFIC AND CULTURAL ORGANIZATION

MIRAMARE-TRIESTE

IC/94/353

International Atomic Energy Agency
and
United Nations Educational Scientific and Cultural Organization
INTERNATIONAL CENTRE FOR THEORETICAL PHYSICS

CRITICAL TEMPERATURES T_c ESTIMATED BY JOSEPHSON-JUNCTION ARRAY MODEL OF LAYERED HIGH T_c SUPERCONDUCTORS[1]

C. Kawabata
Okayama University Computer Center, Okayama 700, Japan,

S.R. Shenoy
International Centre for Theoretical Physics, Trieste, Italy

and

A.R. Bishop
Theoretical Division, Los Alamos National Laboratory, Los Alamos, NM 87545, USA.

MIRAMARE – TRIESTE
November 1994

[1]8th Cimtec Forum on New Materials. Topical Symposium IV (Superconductivity & Superconducting Materials Technologies) Florence, Italy, July 1–4 (June 28–July 4), 1994.

ABSTRACT

We model high T_c superconductors(HTS) by quantum capacitive Josephson junction arrays(JJA), with Angstrom-scale parameters, to obtain an estimate of Tc trends. The basic idea is as follows. Number (or charge) and phase are conjugate variables, with the uncertainty products obeying $\Delta N \cdot \Delta \theta > 1$. Thus, in HTS, global phase coherence is opposed by charging-energy induced quantum phase fluctuations, especially across Josephson-coupled CuO_2 planes. These have separation $d_\perp$ and effective interplanar dielectric constant ε, e.g. from Y atoms in YBaCuO. Decreasing the interplane charging energy $E_{c\perp} \sim d_\perp / \varepsilon$, raises T_c.

In Section 1, we motivate a modelling of HTS phase excitations by a quantum capacitive 3D JJA model, with XY planar phases. Section 2 gives a physical picture of the HTS transition, relating the complex layered HTS structure to a simpler "intermediate level" quantum 3D JJA/XY model. Section 3 sets up a path integral (3+1)D model that reduces to a previously studied anisotropic 3D XY/JJA model, with constants renormalized in some way, by the capacitance. Postponing a detailed analysis to elsewhere, we make a heuristic estimate for the reduction of the previous T_c, by the charging energy.

1. MOTIVATION

The detailed superconductivity mechanism in HTS is unknown, but it will certainly produce a macroscopic wave function $\Psi = |\Psi| \exp(i\theta)$. The magnitude $|\Psi|$ and phase $-\pi < \theta(r) < \pi$, fluctuate above the transition, with the mean magnitude becoming nonzero $<|\Psi|> \sim T_{GL} - T$, below a Ginzburg-Landau temperature T_{GL}. The resistance R(T) falls [1] near T_{GL}, but vanishes, $R(T_c) = 0$, only at a lower $T_c < T_{GL}$, where macroscopic phase coherence sets in. This implies that a special "intermediate level" role is played in HTS, by models with planar phases $-\pi < \theta_i < \pi$, describing the phase coherence transition. These are 3D XY models, with nearest-neighbour energies $\sim \cos(\theta_i - \theta_j)$[2].(Josephson junction arrays [2,3], Fig. , of weakly coupled superconducting grains with superconducting phases $\{\theta_i\}$, have XY-like Hamiltonians, and therefore also play a special role.) Microscopic theory would determine the anisotropic phase coupling constants within ($K_{//}$), and between ($K_\perp$), layers. The anisotropic 3D XY/JJA system can thus model the phase excitations/critical behaviour of HTS, and indeed many HTS properties appear to fall into this universality class [4]. For example, 3D XY critical exponents and scaling behaviour have been observed for HTS [4]. Also,signatures of XY/JJA topological phase excitations (vortices) have been reported, in the R(T) temperature dependence, and in nonlinear I-V curves [5]. These signatures are however,

characteristic of the two-dimensional unbinding of logarithmically interacting vortex points [6], while the 3D XY/JJA topological excitations are vortex loops [7], interacting via a Biot-Savart law. A blowout of the largest loops, of diameter $\xi_{-}(T) \sim (T_c - T)^{-\nu}$, drives the transition [8,9]. The dimensionality puzzle can be resolved by a vortex loop scaling approach [8,9], generalized [10] to the anisotropic case. The results show that:
(i) Anisotropy is irrelevant, and 3D multiplane loops dominate the transition within a critical region estimated as $| (T_c - T)/T_c | < (K_\perp/K_{//})^{1/2\nu}$. (ii) Outside this critical region finite-scale quasi-2D loops cutting single layers, produce 2D-like signatures. (iii) The 3D XY/JJA Tc as a function of the anisotropic coupling ratio $K_\perp/K_{//}$, can be determined from the vortex loop scaling equations. Thus some HTS phase coherence / excitation behavior can be understood through the classical 3D XY/JJA model. The picture is not complete, however: charging energy effects, or quantum fluctuations, must be included [11]. HTS involve strongly correlated electrons, described by Hubbard-like models, that can be related to XY-like models [12]. Even if some mechanism produces local Cooper pairs, Coulombic pair repulsion, that inhibits phase coherence, cannot be ignored. Quantum fluctuation effects on the magnetization, and on vortex-lattice melting have been reported [13]. Systematic variations of Tc with carrier-plane separation d_1 [14], Fig 2 indicate that interplane charging energies $E_{c\perp} \sim d_1$ may play a role. HTS superlattices, alloys, and materials show a T_c variation with capacitance [15,16], as do 2D quantum capacitive JJA [17]. Thus the previous classical 3D XY/JJA vortex loop scaling analysis must be generalized to the quantum case, or in a path-integral formulation, to the classical (3+1)D case. In some physical limit, the previous 3D, and quasi-2D noncritical results must be shown to be recovered. But as a first step, we next justify use of a simple JJA model for HTS in more detail.

2. PHYSICAL PICTURE OF HTS TRANSITION, AND JJA MODEL

The structure of the prototypical HTS material YBaCuO is given in Fig.3a. It may be regarded as composed of two blocks [18], with distinct phase coherence and charging properties [19]. The charge carriers, on CuO_2 planes of square lattice constant $\sim l_0$ (of scale Angstroms), have fractional concentration x per plane. There is a "mediating" [18] or "weak coherence" [19] region of thickness d_1 Angstrom between CuO_2 layers in one unit cell and the next (containing Y atoms). The CuO_2 layers rest on "blocking" or "neutralizing" [18] regions of thickness d_2 Angstroms, containing Ba, apical oxygens, O-deficient CuO_2 chains/planes, etc.. The d_2 neutralizing region compensates the nominal charges on the CuO_2 carrier planes and Y atom layers in d_1, ensuring unit-cell neutrality [18]. (For La compounds, d_1 and d_2 are the same.)

We assume that carriers (on the O sites, say), of average doping density x / l_0^2, $1 > x > 0$, form a local superconducting-pair areal density $n_p = (1/2)\, x / l_0^2 \equiv a_{//}^{-2}$, below some T_{0t}, through some superconductivity mechanism. The carrier-pairs, for $T_{0t} > T > T_c$, are pictured as locally phase-coherent "patches", clumped into areas $a_0^2 \sim \pi \xi_{//}^2$, where the in-plane GL coherence length is $\xi_{//} > l_0$. The distance

between patch centers is the in-plane lattice constant $a_{//} = n_p^{-1/2}$. The separation between the patch edges, across which the local pairs must tunnel to establish coherence, is $w = a_{//} - a_0 = a_0[(x_c/x)^{1/2} - 1]$, where $x_c \equiv 2(l_0/a_0)^2$, < 1 [19]. See Fig.3b. For $l_0 = 3$ Å, $\xi_{//} \simeq 13$ Å, one has $x_c = 0.04$.

Each patch has a phase θ_i associated with it, from the local coherence wave function $\Psi_i = |\Psi_i| \exp(i\theta_i)$. Neighbouring patches are Josephson-coupled : intraplane (interplane) across w (d_1) through coupling $E_{J//}(w)$ ($E_{J\perp}(d_1)$). The couplings $E_{J//}(w) \equiv E_{J//}(0)I_{//}(w)$ and $E_{J\perp}(d_1) \equiv E_{J\perp}(0)I_\perp(d_1)$ depend on separations w and d_1 through overlap integrals $I_{//}(w)$ and $I_\perp(d_1)$, estimated later. (The zero-separation normalization is $I_{//}(0) = I_\perp(0) = 1$, with $I_{//}(w(x))$ set to unity for $x > x_c$.) The patches are generated by some "pumping structures", and may be thought of as localized beneath them, making an in-plane lattice plausible. However, this is not an essential part of the argument; a continum in-plane limit is certainly appropriate for large distances, and large doping, $x > x_c$. For typical HTS parameters $x_c \sim 0.04$. The average (and hence continuous) charge on a patch is $q = 2e\, n_p\, a_0^2 = 2e\,(x/x_c)$, where for $x = x_c$, the fluctuating-charge patch regions contain one Cooper pair,on average. The interpatch parallel-plate capacitance across d_1 is $C_J = \varepsilon\, a_0^2 / 4\pi d_1$, yielding a charging energy

$$E_{c\perp} = q^2 / C_J = \pi (4ex/x_c a_0)^2\, d_1/\varepsilon \qquad (1)$$

Here ε is the weak coherence region's effective dielectric constant, dependent on the atomic polarizabilities in d_1 (Y in Fig.3a). We neglect charging energies between in-plane patches, valid especially, for $w / a_{//} << 1$, or $x \sim x_c$. (Note that we are interested only in dynamic changes in local charge, and neglect throughout the fixed background nominal ionic charges [18] in the unit cell.)

What about phase coherence and charging energies across the neutralizing region d_2? We assume charge transfer/phase locking across d_2 is faster than across d_1. Thus, over the time scales set by d_1 processes, (i) the patch phases joined by vertical dashed lines in Fig.3b, can be treated as locked together ; (ii) there is no appreciable charging energy across them. The pumping structures in the vertical dashed lines effectively act as "superconducting cylinders" with patches on their circular faces, of fixed phase and negligible charging energy. In other words, near T_c, the d_2 region maintains its neutralizing role, even for dynamic charge transfer processes between unit cells.

To place these ideas in a broader perspective, the following picture of the HTS transition is suggested [19]. For $T > T_c$, the local pairing patches are phase-incoherent within, and between planes. They are visualized as flickering in and out of existence, locally driven by d_2 pumping structures [20,21] with uncorrelated oscillation phases. For $T < T_c$, global phase coherence begins to set in. The time scale of in-plane patch fluctuations decreases as coherence sets in, consistent with NMR results below T_c [22]. The pair-transfer processes and phase lockings between unit cells, required for the establishment of global phase coherence, become slow variables, that dynamically slave the fast charge / elastic degrees of freedom in d_2, linstead of the other way around. The local

adaptive dynamic processes could include [20,21] charge-transfer modes / oxygen two-level flips / interplane buckling adjustments. Thus at T_c, oxygen oscillations are reduced and globally correlated; plane vibrations settle down to a well-defined buckling pattern [23], and a mean d_1 with steady interplane pair tunneling. There is a single T_c at which 3D phase coherence is simultaneously established [24,10], within and between planes. Returning to our model, we see that the d_2 region of Fig.3b collapses as far as slow phase and charge variables are concerned into a JJA layer,with a coherence energy $E_{J//}$ parametrizing its complex physics.(Fig.3c) Tunneling across d_1 is described by the Josephson coupling $E_{J\perp}$. The HTS is modelled by an anisotropic 3D XY/JJA Hamiltonian, Fig.3d, as far as the onset of phase coherence is concerned.

3. THE (3+1)D XY/JJA HAMILTONIAN

The classical (anisotropic) 3D XY/JJA model [7] of Fig.3d is ($\beta = 1/k_B T$)

$$\beta H_{cos}(\{\theta_i\}) = -\sum_{\mu=\hat{x},\hat{y},\hat{z}} \sum_i K_\mu \cos(\Delta_\mu \theta_i) \qquad (2)$$

where Δ_μ is a discrete derivative in directions $\mu = x,y,z$; {i} are superconducting grain (phase) sites on a cube lattice; $\{\theta_i\}$ are phase variables $-\pi < \theta_i < \pi$, and dimensionless layered couplings are $K_x = K_y \equiv K_{//} = \beta E_{J//}$, $K_z \equiv K_\perp = \beta E_J$. The layered JJA model may be regarded as a Ginzburg-Landau-Lawrence-Doniach model [25], discretized in-plane, for convenience of discussion. The couplings $K_{//}$, $K_\perp$ are related in the GL picture to anisotropic penetration depths, $K_{//,\perp} \sim \lambda_{//,\perp}^{-2}$. The anisotropic coupling ratios are GL mass ratios $K_\perp / K_{//} = m_{//} / m_\perp \equiv \gamma_0^{-2}$ [25,10]. To generalize Equ(2) to include quantum fluctuations, we add "kinetic energy" terms [3,17] involving number operators $\hat{N}_i = (\hbar/i)d/d\theta_i$, canonically conjugate to the phase θ_i. These are the charging energy operators $(2e)^2 \sum \hat{N}_i^2/2C_0$ where C_0 is the grain capacitance. Similar terms are added for intergrain capacitance C_J. In a path integral formulation, analogous to the 2D case, [17], the quantum 3D JJA model can be written as a (3+1)D XY/JJA model. An imaginary time variable τ provides the extra dimemsion, $\theta_i \rightarrow \theta_i(\tau)$. Thus the action or "Hamiltonian" is

$$S = '\beta H' = \int_0^{\hbar} d\tau \, [H_{cos}(\{\theta_i(\tau)\}) + H_0] \qquad (3a)$$

where the charging energy contributions are

$$H_0 = (1/2)m \sum_i (\dot{\theta}_i(\tau))^2 + (1/2)M_\perp \sum_{<ij>}{}' (\dot{\theta}_i(\tau) - \dot{\theta}_j(\tau))^2 \qquad (3b)$$

The dot denotes a "time" derivative. The prime on the second, intergrain charging term in Equ(3b) means that the sum is only between nearest-neighbor grains ("patches" in Fig 3c) on different layers, across the d_1 distance. The masses are related to (twice the)

charging energies by [26] $m=\hbar^2/E_{c0}$, $M_\perp=\hbar^2/E_{cJ}$, where $E_{c0}=(2e)^2/C_0$ and $E_{cJ}=(2e)^2/C_J$, and is $E_{c\perp}$ of Equ(1) in this case. We need to generalize the 3D vortex-loop scaling analysis [10] to the (3+1)D XY/JJA model of Equ(3), where the topological excitations are possibly vortex tubes / toroids [27]. However, we do not pursue this here. We note, instead that Equ(3) is like an extended boson-Hubbard model [28], with boson magnitudes locked in a coherent state representation. The on-site charging energy $m^{-1}\sim E_{c0}$ is like a Hubbard "U", while $M_\perp^{-1}$ is like an intersite Coulomb "V". The large "U" limit is of interest. Expanding Equ(3b) in a small wave-vector/frequency spinwave approximation, ($a_x=a_y=a_{//}$, $a_z=d_\perp$),

$$H_0 \approx 1/2\sum_{\vec{q},\omega}\Big[\sum_{\mu} E_{J\mu}q_\mu^2 a_\mu^2 + m\omega^2 + M_\perp[\vec{q}_{//}\omega]^2\Big]\,|\,\theta_{\vec{q},\omega}\,|^2 \qquad (4)$$

The first term$\sim m\omega^2$ increases the model's effective dimensionality, from 3D to (3+1)D. The $M_\perp q^2\omega^2$ term is formally of higher order, and can only be important at finite scales, $<(M_\perp/m)^{1/2}a_{//} = (E_{c0}/E_{c\perp})^{1/2}a_{//}$. Suitable rescaling yields a temperature-dependent "box size" in the τ direction, or quantum scale, $r_0\equiv[(E_{c0}E_J)^{1/2}/k_BT]a_{//}$. Thus the system is (3+1)D only at T=0; at any nonzero T, the asymptotic behavior and critical exponents, are those of a 3DXY model[4,10]. Finite-scale quantum effects can at most, affect T_c, and noncritical behavior. For $M/m >>1$, the $M_\perp q^2 a_{//}^2\omega^2$ term dominates the $m\omega^2$ term over most of the finite-scale region $< r_0$. (With E_J, $E_{c\perp}\sim 10^{3\circ}$ K, $T_c\sim 10^{2\circ}$ K, and $C_0\sim a_0\sim\xi_{//}\sim 10$ Å, one has $E_{c0}\sim 10^{5\circ}$ K, while $r_0/a_{//}\sim 10^2$. In the range $2\pi/r_0 < q < 2\pi/a_{//}$, the ratio of the capacitive terms is in the range $1<(M/m)q^2a_{//}^2<4000$. Thus $m\omega^2$ is dropped, $m\sim E_{c0}^{-1}\to 0$, in a large "U" limit, and quantum corrections mostly come from $M_\perp\sim E_{c0}^{-1}$. The transition temperature in this limit will be that of the 3D vortex loop case, reduced by the charging energy, $T_0 = T_c(E_{c\perp})$

We next make a simple, back-of-envelope estimate of T_c, deferring a more detailed analysis to elsewhere.

4. T_c ESTIMATE

For charging energy $E_{c\perp} = 0$, a vortex-loop scaling analysis of the classical anisotropic 3D XY/JJA model yields the dimensionless critical coupling in terms of the coupling anisotropy, as [10]

$$E_J/k_BT_c = 0.454\, f(\gamma_0^{-2},0) \qquad (5)$$

Here $f_0\equiv f(\gamma_0^{-2},0)$ is determined from scaling equations. One finds $f_0 \to 1$ for isotropy, $\gamma_0^{-1} = 1 = E_{J\perp}/E_{J//}$, while $f_0 \to 2\ \gamma_0^{-1}$ for decoupled planes $\gamma_0^{-1}\to 0$, recovering the KT transition temperature [10]. E_J is an effective isotropic coupling, defined by the geometric mean, [10,29]:

$$E_J \equiv \sqrt{E_{J//}(w)E_{J\perp}(d_\perp)} \qquad (6)$$

From GL mass ratios, $\gamma_0^{-1} \sim 0.02$ for thallium, and ~ 0.2 for yttrium compounds [10,25]. A generalization of the dimensionless critical coupling expression of Equ(5) can

include charging energies only through the ratio of $E_{c\perp}$ and the other available energy E_J. Thus,

$$E_J/k_B T_c = 0.454\, f(\gamma_0^{-2}, E_{c\perp}/E_J) \qquad (7)$$

Here the unknown function on the r.h.s of Equ(7) must reduce to the known Equ(5) for zero charging energy. The leading correction is estimated by Taylor-expanding to leading order, $f(\gamma_0^{-2}, E_{c\perp}/E_J) \approx f_0 + f_0' E_{c\perp}/E_J$. This expression can be adapted to materials [1] with N extra CuO_2 planes (of separation d_1, say) intercalated in the weak coherence region of the unit cell of Fig.3a. The kinetic energy terms of Equ(3b) are like imaginary time "voltages", by analogy with the Josephson relation $\dot{\theta} = 2eV/\hbar$, and generate phase-slips, that nucleate coherence-destroying vortex excitations. For a given inter-unit-cell "voltage" between the outermost CuO_2 layers, the "voltage"-drops across the intercalated layers will be partioned down by a factor $\sim 1/(N+1)$. There will be less quantum fluctuation energy available across any one pair of layers, to nucleate vortices. The N=0 result above can be taken over, with an effective reduction factor in the charging energy between any two planes, $E_{c\perp} \rightarrow E_{c\perp}/(N+1)$.

The final T_c estimate is , from Equ(7)

$$k_B T_c = 2.2(E_J/f_0)[1+E_{c\perp}/E_J(N+1)]^{-1} \leq 1.1 E_{J//} \qquad (8)$$

where for simplicity, we have set the unknown, order-unity Taylor coefficent ratio $f_0'/f_0 = 1$. The quantum fluctuation energy of Equ(1) for typical parameters is $\sim 1000^\circ$ K. The coherence energy E_J must be of the same order, to produce an appreciable T_c. Fig.4 shows the quasi-universal [15,19] curve of scaled T_c versus scaled charging energy. For parameters as below, $E_{c\perp}/E_J = 9.2$, as marked. To raise T_c, one must creep up along the curve, by material tailoring. An upper bound to T_c is set by the coherence energy $E_{J//}$ produced by mechanisms in the d_2 region.

The coherence energy E_J will depend on the overlap integrals for intra/interplane tunneling:

$$E_J = E_J(x,w,d_1) = (x/x_c)^{1/2}\, z(w,d_1) k_B T_J \qquad (9)$$

where $z(w,d_1) \equiv I_{//}(w) I_\perp(d_1)$ is an overlap-integral factor [30].

A coherence energy scale is defined, $k_B T_J \equiv E_J(x_c, w(x_c)=0, d_1=0)$ that is a (high) upper bound for E_J. Atomic-scale pairs are pictured as tunneling through atomic-scale barriers; the mixed valency of copper facilitates such tunneling. A Cooper pair Josephson-tunnels coherently, like a single electron. Thus we (crudely) estimate $I_{//}(w)$, $I_\perp(d_1)$ by overlaps of $d(x^2-y^2)$, $d(z^2)$ copper wavefunctions, separated by w, d_1. Fig.5 shows the separation dependences. To get an idea of magnitudes and trends, we write Equ(8) in terms of scaled parameters, extracting typical scales: $\bar{d} = d_1/3$ Å , $\bar{l}_0 = l_0/3$ Å , $\bar{x}_c = x_c/0.04$, $\bar{\varepsilon} = \varepsilon/10$, $\bar{T}_J = T_J/1000^\circ$ K, and $\bar{x} \equiv x/x_c$. Then, Equ(8) becomes

$$T_c(^\circ\ \mathrm{K}) = 2200(\bar{x}^{1/2} z \bar{T}_J/f_0)/[1+(5.51\bar{d}\bar{x}^2\bar{x}_c/\bar{l}_0^2\bar{\varepsilon}(N+1))/\bar{x}^{1/2} z \bar{T}_J] \qquad (10)$$

The charging energy suppresses T_c from its upper bound, set by the coherence energy. For parameters $\bar{d} = \bar{\varepsilon} = \bar{l}_0 = \bar{x}_c = \bar{x} = 1$, $E_{c\perp} = 5500^\circ$ K, with a choice $T_J = 4000^\circ$ K, and since $z \sim 0.15$, from Fig.5, we get $T_c = 128^\circ$ K. We now plot out

T_c (x,$d_\perp$,N); parameters not explicitly varied , in each case have barred versions set to unity, and we set f_0 = 1. Fig.6 shows T_c versus x for different $d_\perp$, N. T_c rises with zero slope as $\sim x^{1/2}\ \exp(-1/\sqrt{x})$, since interpatch tunneling within planes increases with x, and carriers participating in coherence also increase. (T_c becomes appreciable only near $x = x_c$, when there is on average one Cooper pair per patch.) It falls, as $\sim x^{-1}$ when the charging energy $E_{c\perp} \sim x^2$ starts destroying phase coherence. There is a peak in T_c at $x=x^*(d_\perp,N) > x_c$, arising from these competing tendencies. If we had kept higher order $E_{c\perp}$ terms in Equ(8), T_c would fall faster. Fig.7 shows that T_c rises, and tends to level off, with intercalated layers N, for different $d_\perp$, x values. Fig.8 shows T_c increases as interlayer spacing $d_\perp$ decreases, with a quasilinear region, [14] similar to Fig.2. For large $d_\perp$, T_c falls like $1/d_\perp$, consistent with estimated trends [18]. The previous empirical interlayer systematics [14,18] is now seen as a charging energy dependence $E_{c\perp} \sim d_\perp/\epsilon$ of T_c. External pressure would tend to decrease $d_\perp$ and hence increase T_c (small atoms are like internal pressure [1], in this regard.) Large pressures could cause saturation or a fall in T_c, depending on how the dielectric constant or atomic polarizability varies. The basic message we can conclude is that T_c can be raised in two ways: (i)By optimizing the complex chemical and physical processes in the neutralizing d_2 region, so as to raise the coherence scale $E_{J//}$, that is an upper bound for T_c. (ii) By reducing quantum fluctuations $E_{c\perp} \sim d_\perp/\epsilon$ in the weak coherence $d_\perp$ region, (smaller, and more polarizable interlayer atoms), so as to move closer to the intrinsic upper bound. In summary, critical temperature trends have been estimated through modelling high temperature superconducting materials by quantum capacitive Josephson junction arrays. Further work will include detailed parameter fits;exploration of mechanisms consistent with the physical picture that motivated the model; (3+1)D XY simulations; and a (3+1)D generalization of vortex−loop scaling.

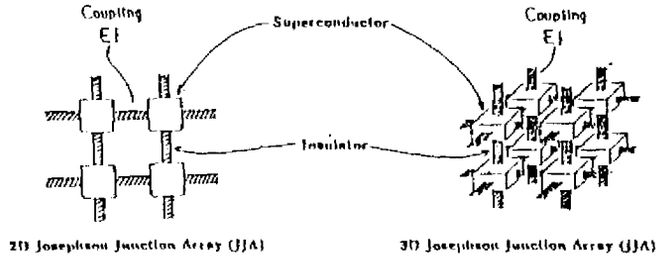

FIGURE 1
Josephson junction arrays in 2D and 3D.

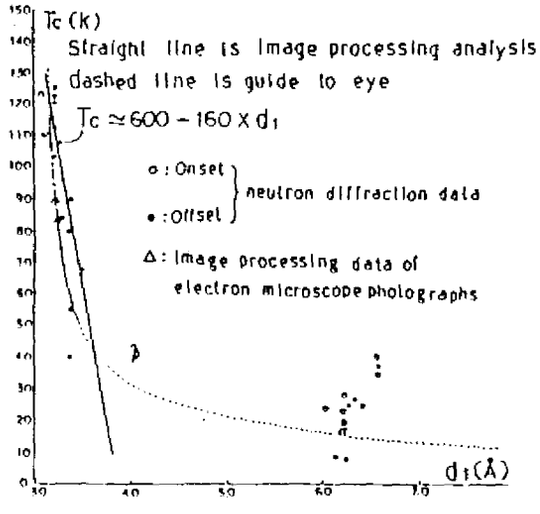

FIGURE 2
Empirical transition temperature variation with interplane separation $d_\perp$, from Ref 14.

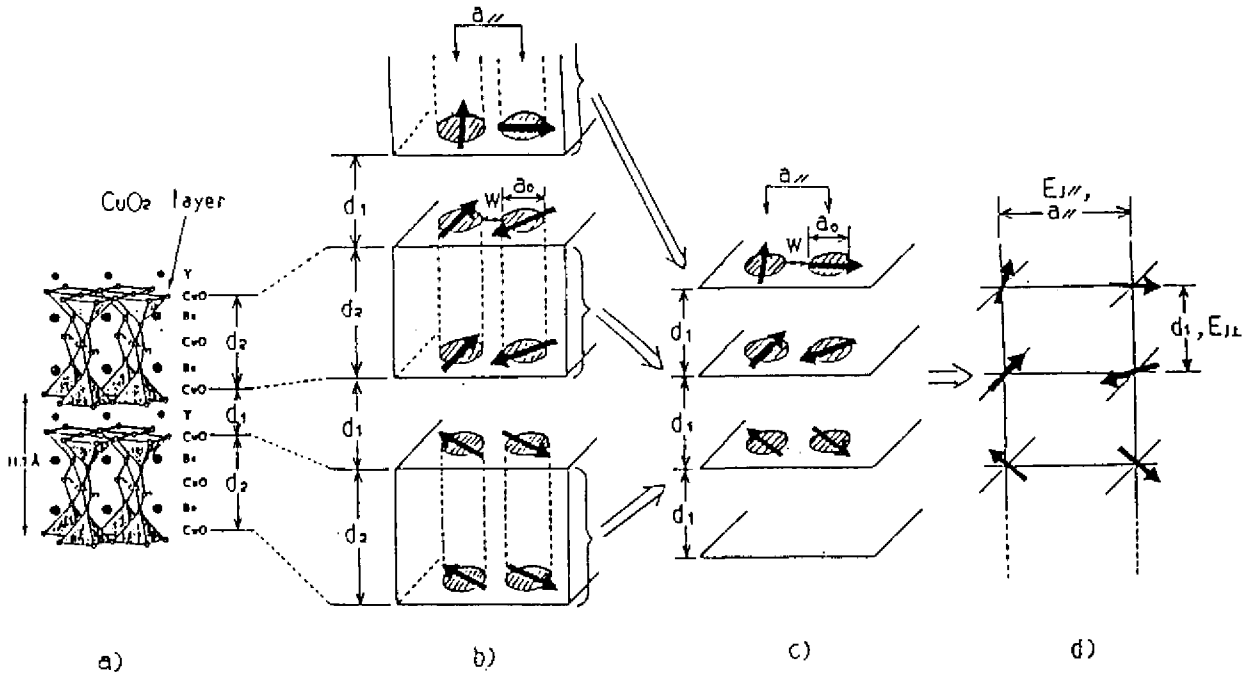

FIGURE 3
a) YBaCuO structure, showing d_2 neutralizing region, and d_1 weak coherence region.
b) Postulated superconducting "patch" and phase, variation. Note phase–locking on patches bracketing vertical dashed lines: see text. The distance between patch centers (edges) is $a_{//}(w)$, while a_0 is the scale of a patch.
c) Effective JJA structure, with d_1 region between planes.
d) Final XY/JJA model of HTS.

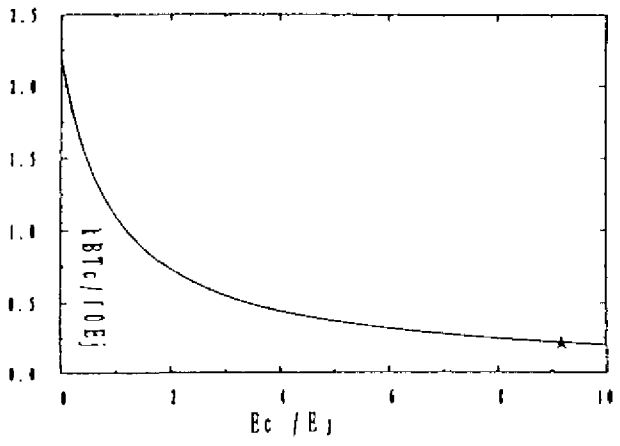

FIGURE 4
Dimensionless plot of scaled transition temperature versus scaled charging energy, with star denoting values for typical parameters, in the text.

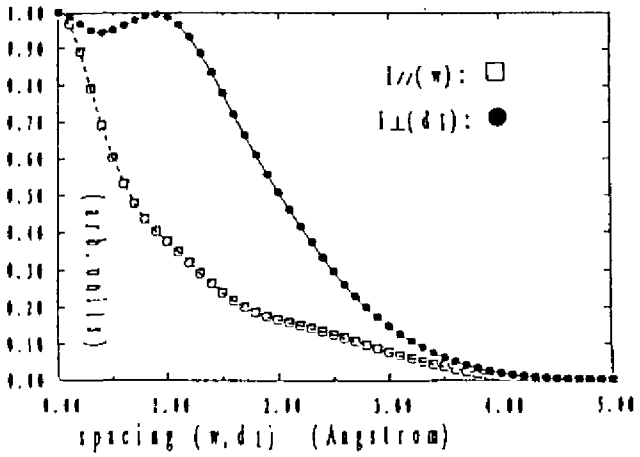

FIGURE 5
Overlap integrals $I_{//}(I_{\perp})$, within (between) planes, versus in–plane patch edge separation w (interplane separation d_1).

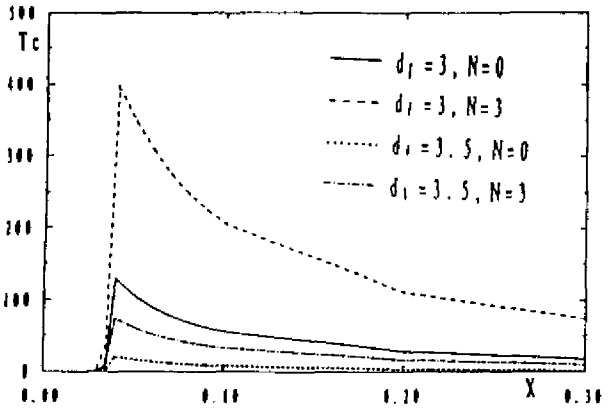

FIGURE 6
Transition temperature versus carrier fraction,x, for different interplane distances d_I, and extra intercalated planes N.

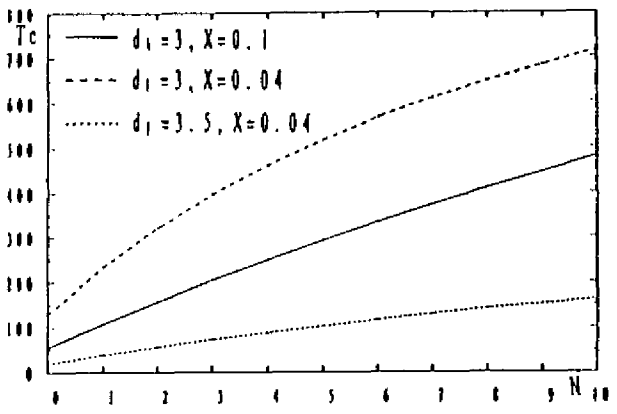

FIGURE 7
Transition temperature versus number of intercalated planes N, for different interplane separation d_I, and carrier fraction x.

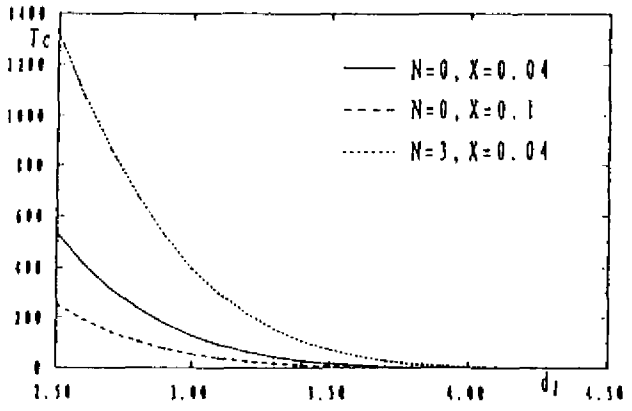

FIGURE 8
Transition temperature versus interplane separation d_I, for different carrier fraction x, and intercalated planes N.

REFERENCES

1) High Temperature Superconductivity, G.Burns, Academic Press,(1992).

2) C.J.Lobb,Physica B+C 152(1988)212, Proc.of Delft Workshop on Coherence in Superconducting Networks; S.R.Shenoy, Troise'me Cycle de la Physique, Lecture Notes on Josephson Junction Arrays, Neuchatel,(1989).

3) B.Abeles,Phys.Rev.B15(1977)2828;P.W.Anderson, in "The Manybody Problem " Vol.II, ed.E.Caianello, Academic, NY,(1969).

4) M.B.Salamon, J.Shi, N.Overend, M.A.Howson, Phys.Rev.B43(1994)5520; N.Overend, M.A.Howson, and I.D.Lawrie, Phys.Rev.Lett.72(1994)3238; T.Schneider,Int.J.Mod.Phys.B,8(1994)487.

5) S.Martin, A.T.Fiory,R.M.Fleming,G.P.Espinosa, and A.S.Cooper, Phys.Rev.Lett.62(1988)677 and references therein.

6) J.M.Kosterlitz and D.J.Thouless, J.Phys.C6(1973)1181.

7) R.Savit,Phys.Rev.B17(1978)1340;Rev.Mod.Phys.52(1990)453.

8) G.A.Williams,Phys.Rev.Lett.59(1987)1926;Physica,165(1990)769; Phys.Rev.Lett. 68(1992)2054;J.Low.Temp.Phys.,89(1992)91;Phys.Rev.Lett.71(1993)392; Physica B194(1994)1415.

9) S.R.Shenoy,Phys.Rev.B40(1989)5056;Phys.Rev.B42(1990)8595; Helv.Phys.Acta,65(1992)477; Current Science(Bangalore),65(1993)392.

10)B.Chattopadhyay and S.R.Shenoy, Phys.Rev.Lett.72(1994)400 and Phys.Rev.B(submitted).

11)D.Harshmann and A.P.Mills, Phys.Rev.B45(1992)10684.;B.Batlogg,Physics of High Temperature Superconductors,Springer(1992)p.219.

12)D.Schmeltzer and A.R.Bishop,Phys.Rev.B41(1990)9603;N.Nagaosa,Phys.Rev.Lett. 71(1993)4210.

13)L.N.Bulaevskii, et.al., preprint, LA UR 93−2758; G.Blatter and B.Ivlev, Phys.Rev.Lett.70,(1993),2621.

14)C.Kawabata and T.Nakanishi,J.Phys.Soc.Jpn,61(1992)466;Symposium III, IUMRS−ICAM93,Tokyo,to bepublished, Elsevier.

15)D.Ariosa and H.Beck, Phys.Rev.B43(1991)344; D.Ariosa, T.Luthy, V.Tsanera, B.Jeanneret, H.Beck, and P.Martinoli, Physica B194,(1994),2371.

16)Y.Matsuda, S.Komiyama, T.Onogi, T.Terashima,K.Shimura and Y.Bando, Phys.Rev.B48(1993)10498.

17)L.J.Geerligs and J.E.Mooij, Physica, B+C, 152(1988)212; R.Fazio and G.Schoen,Phys.Rev.B43(1991)5507.

18)H.Nobumasa,K.Shimizu and T.Kawai,PhysicaC167(1990)515;Z.Phys.B83(1991)7; H.Nobumasa,K.Shimizu,M.Nishina and T.Kawai,Z.Phys.B90(1993)387.

19)C.Kawabata,S.R.Shenoy and A.R.Bishop,Proc,ETL Workshop on HTS,Bull.of Electrotechnical Laboratory,58(1994)17.

20)Proc.Conf.on lattice Effects in High Tc superconductors, Santa Fe, Jan., 1992, ed.Y.Bar−Yam, T.Egami,J.Mustre−de Leon and A.R.Bishop,World Scientific(1992).

21)I.Batistic,A.R.Bishop,R.L.Martin and Z.Tesanovic, Phys.Rev.B40(1990)6896; N.Plakida,V.L.Aksenovic and S.L.Drechsler,Europhys.Lett.4(1987)1309.

22)Y.Wu,S.Pradhan and P.Boolchand, Phys.Rev.Lett.67(1991)3184.

23)R.P.Sharma,L.E.Rehn,P.M.Baldo and J.Z.Liu,Phys.Rev.Lett.62(1989)2869.

24)S.E.Korshunov,Europhys.Lett.11(1990)757.

25)R.A.Klemm,A.Luther and M.R.Beasley,Phys.Rev.B12(1975)877 and refs therein;K.H.Fischer,Physica C210(1993)179;R.Kleiner and P.Muller,Phys.Rev.B49 (1994)1327.

26)U.Eckern and A.Schmid,Phys.rev.B39(1989)6441.

27)G.A.Goldin, R.Menikoff, and D.H.Sharp, Phys.Rev.Lett.,67,(1991),3499.

28)K.Sheshadri,H.R.Krishnamurthy,R.Pandit and T.V.Ramakrishnan,Europhys. Lett.22(1993)257.

29)W.Janke and T.Matsui,Phys.rev.B42(1990)10673.

30)The Josephson coupling $E_J(\Delta)$ goes as Δ at low temperatures and as Δ^2, the superfluid density, near transition. Since $T_c << T_{GL}$ for magnitude locking, and with superfluid density $n_s \sim x \sim \Delta^2$, we take the low temperature form, $E_J \sim x^{1/2}$. In Ref 19, for x rising from small values, we neglected this dependence compared to the sharply rising overlap integral $I_{//} \sim \exp(-(x_c/x)^{1/2})$. The T_c curves are qualitatively unchanged.